On Reducing the Post-Heat-Treatment Time of the Weldment

S. Jahanian, R.R. Kunde, and P.V. Kuppa

(Submitted 1 May 1998; in revised form 5 April 1999)

Post heat treatment of weldments is one of the most extensively used techniques by the industrial community for relieving welding residual stresses. Such practice not only delays the manufacturing process, but also increases the cost of manufacturing. In this article, an idea of a new welding technique, which is a promising tool for relieving welding residual stresses, is presented. This method is anticipated to reduce the time and cost of the manufacturing process. The first part of the investigation focuses on simulation of an idea by using an auxiliary heat source for creating a weldment with a more uniform temperature distribution both spatially and temporally. A subroutine has been developed for optimizing the size of an auxiliary heat input (AHI). The details of the subroutine and the parameters considered for optimizing the AHI are presented. The results show that by increasing the stabilizing temperature and size of the AHI, the speed of cooling and spatial temperature gradient decreases. This may result in reducing the level of residual stresses.

Keywords post treatment, residual stress, welding

1. Introduction

Development of undesirable residual stresses and low fatigue life of a welded structure has been a major concern to welding engineers. In recent years, several techniques have been proposed to reduce or partially eliminate the undesirable residual stresses in the weldment.[1,2]

Recently, Lin and co-workers[3–7] developed the parallel heat welding (PHW) technique for reducing undesirable residual stresses in the weldments. In their experimental model, an auxiliary heat source moved parallel to and at the same speed as the welding torches. This technique has been developed for reduction of residual stresses in stainless steel. When the technique was originally tested on stainless steel,[3–5] 21 to 32% reduction of residual stresses was reported. Later, Chang and Chou[6] reported 11.5 to 26.2% reduction of residual stresses for AISI 316 stainless steel. Recently, Lin and Lee[7] used a similar method on AISI 304 and investigated the effect of welding parameters on the residual stresses. They reported that the level of residual stresses had been increased.

All the work that has been reported was experimental,[3–7] and a solid conclusion of how to optimize such a welding technique was never made by the authors of the aforementioned papers. By carefully scrutinizing the temperature distribution curves of their work, one can clearly detect a region of thermal shock as well as a high spatial temperature gradient (Fig. 4 to 6 in Ref 7) at the surface of the weldment.

Residual stresses are generally developed in the weldment as a result of uneven heating and cooling in and around the weldment. By reducing the speed of cooling and spatial temperature gradient, one may reduce the level of residual stresses.[8,9,10] Recently, Kundue *et al.*[11] showed that spatial and temporal temperature gradients in the weldment may be reduced when auxiliary heat input (AHI) is properly selected. In their analysis, the AHI has been selected based on trial and error. In this article, a systematic study is undertaken to investigate the effect of an AHI on the temperature distribution and on the residual stress distribution. This heat input, normally used in parallel heat welding, is applied on the top surface of the weldment.

Initially, an AHI is introduced, similar to the work of Ref 12, then a subroutine is used to optimize it. This not only minimizes the spatial temperature gradient around the heat-affected zone (HAZ), but also reduces the speed of cooling of the weldment and develops a more uniform speed of cooling around the HAZ. By developing such a situation, the level of residual stresses is expected to be reduced.

2. Numerical Approach

Two annealed grooved plates of 0.152 by 0.152 by 0.025 m (6 by 6 by 1 in.), similar to the experimental setup of Shim,[12] are considered. Using gas metal arc welding, the plates were joined together.[12] The temperature distribution on the surface of the plate was evaluated using the ABAQUS finite-element model code. A reasonable agreement between the numerical analysis and the experimental results of Shim is observed (Fig. 1). The model, along with the boundary conditions used, is discussed in the following sections.

2.1 The Model

To model the process of welding, a cross section of a 0.025 m (1 in.) thick plate is considered. At this cross section, it is assumed that there is symmetry along the centerline. This assumption can be justified if one thinks that the weld torch is held exactly at the centerline (*i.e.*, right over the middle of the notch). Therefore, it gives an equal amount of heat to both sides of the centerline. The AHI is also applied on both sides of the centerline

S. Jahanian, R.R. Kunde, and P.V. Kuppa, Department of Mechanical Engineering, Temple University, Philadelphia, PA 19122. Contact e-mail: jahanian@astro.temple.edu.

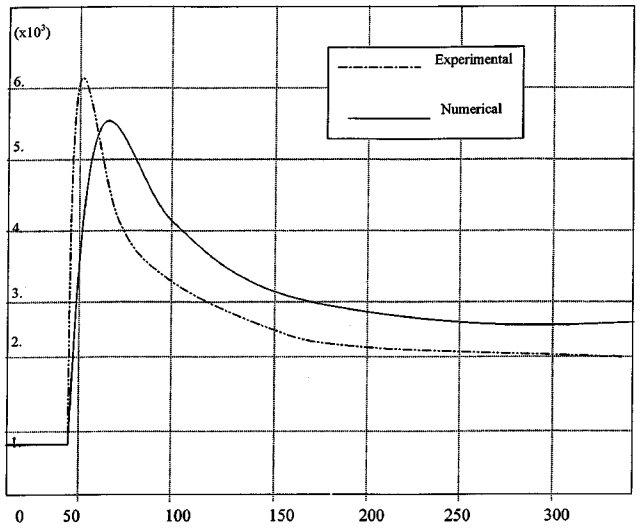

Fig. 1 Experimental verification

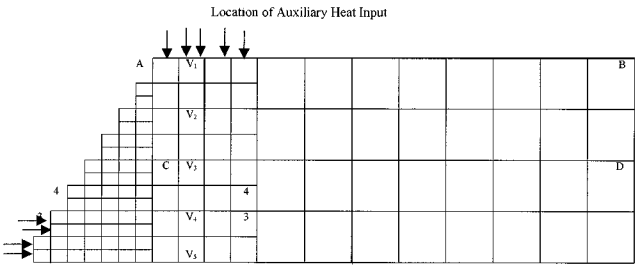

Fig. 2 Locations of the AHI and welding heat input. Three analyses have been performed: **(a)** AHS = 0 in., **(b)** AHS = 1 in., and **(c)** AHS = 1.5 in.

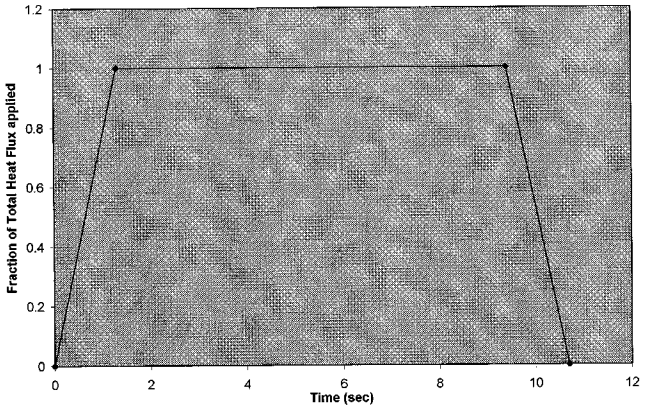

Fig. 3 Ramp function used for welding heat input

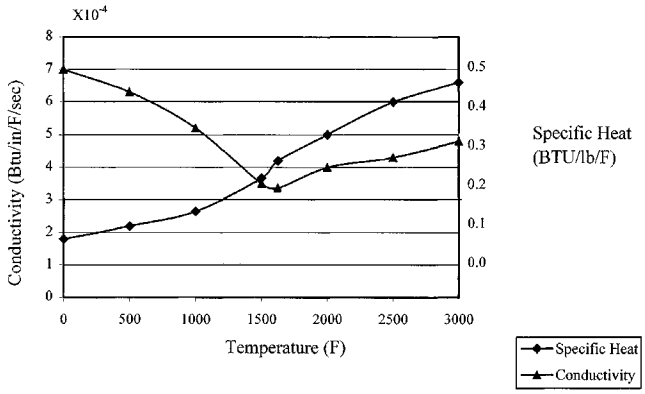

Fig. 4 Thermal properties of AISI 3041 steel

symmetrically. Geometrically, it is known that the cross section is symmetrical about the centerline.

Eight-noded quadrilateral heat transfer elements are considered to model the cross section of the plate. The total number of nodes used is 649, the elements are 192, and the total degrees of freedom the model possesses is 649. The mesh and location of the AHI are depicted in Fig. 2.

Welding Heat Input. To model the heat input, a ramp function is used. This assumes that the value of heat flux, which is applied to the weldment, increases with time linearly as a ramp. Two factors are considered when selecting this type of function.

- it reduces the sudden jump in temperature at any particular node, between the time steps (this is to avoid the numerical convergence problem); and
- it represents the physical situation of simulating the effect of a moving arc more closely than a sudden input of heat flux, (although a closer representation could be a Gaussian curve, for the sake of simplicity, a ramp is considered).

A linear rise in the value of the heat input is taken, until it reaches its maximum in 10% of the total time applied. This value stays at the peak for 90% of heat input time, and then, in the last 10% of the time, it reduces linearly to reach zero (Fig. 3). A distributed heat flux is applied as the thermal load throughout the element face.

The **boundary conditions** used with the heat input for various situations are as follows.

- Convection heat transfer takes place at the top, sides, and bottom surface of the weldment.
- Heat input by the weld bead (for the first pass) is shown at the left corner of Fig. 2.
- The problem is first solved using the above boundary condition, later on, AHI is introduced at the area shown in Fig. 2.

Numerical Data. For the purpose of comparison with experimental data, the following data from Shim[12] are used:

- thermal properties: assumed to be a function of temperature, as shown in Fig. 4;
- the maximum heat input for welding torch: 2.518 kg/s^3 (15.4 Btu/in.^{2}/s) for 3.175×10^{-3} m (0.125 in.);
- thickness of plate: 0.025 m (1.00 in.); and
- film coefficient for convection: 9.085 kg/s.s. · K (1.0×10^{-5} Btu/in.^{2} · °F).

3. Proper Selection of the AHI

As a first step, the AHI was assumed to move at the same speed as a welding torch, similar to Li and co-workers' experiments.[3–7] As a result of this, a thermal shock was introduced into the plate (Fig. 5a). A high spatial temperature gradient was also observed at the surface and along the thickness of the plate. At this point, the following a criteria were arrived at for selection of the AHI:

- the temperature gradient across the thickness of the plate must be minimum;
- the temperature gradient across the top, middle, and bottom rows must be minimum;
- the temperatures at the areas where the AHI is applied, and areas adjacent to it, must reach their peaks at the same time;
- the speed of cooling must be reduced and should be uniform; and
- the AHI must be selected based on a predefined stabilizing temperature.

In the process of optimization of the AHI, the subroutine was developed depending on the above criteria and is discussed in the next sections.

3.1 User Subroutine

The AHI is defined by certain parameters such as magnitude, length of application, starting time with respect to welding heat input, and ramp function. This subroutine explains how one can determine these parameters and arrive at an optimal AHI for a given welding heat input. In the process of determination of these parameters, data at certain critical sections such as AB, CD, and across V_1–V_5 (Fig. 2) are collected and used as representative data for the analysis.

Step 1: Magnitude of the AHI. Twenty percent of the magnitude of the welding heat input is assumed to be the initial value of the magnitude of the AHI. The procedure followed to arrive at an optimum value of AHI magnitude involves iterative incrementation of the initial value of magnitude while checking for the minimum spatial temperature gradient *dT* for every increment along AB. In all the cross sections considered, that section that is midway to the application of the AHI was found to be ideal for analyzing the data for magnitude of the AHI. The section AB is situated across the center of where the AHI is located and is considered to be representative of all the cross sections. $dT = T_A - T_O$ is the spatial temperature gradient between point A and the other nodes along AB (Fig. 2), when the temperature at point A reaches its peak. Depending upon *dT*, the value of the magnitude obtained after every increment is either incremented or decremented, minimizing the difference *dT* until a predetermined value of convergence is reached. If an overshoot occurs (in any direction), one increment is deducted and an increment of one-tenth of the last increment is used, until the desired degree of convergence is obtained.

Step 2: Length of Application of the AHI. The determination of the length over which the AHI is applied depends on the

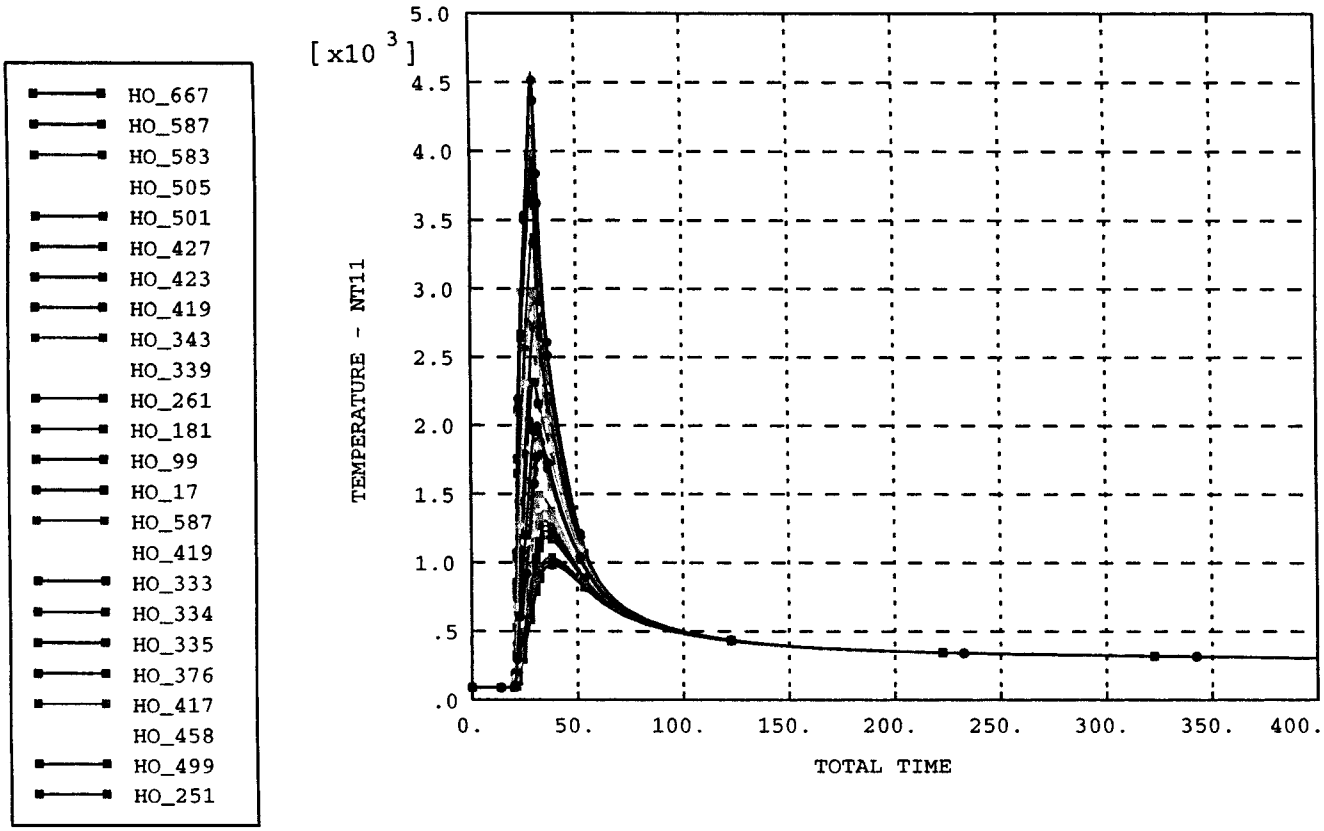

Fig. 5 Temperature distribution: **(a)** in the HAZ

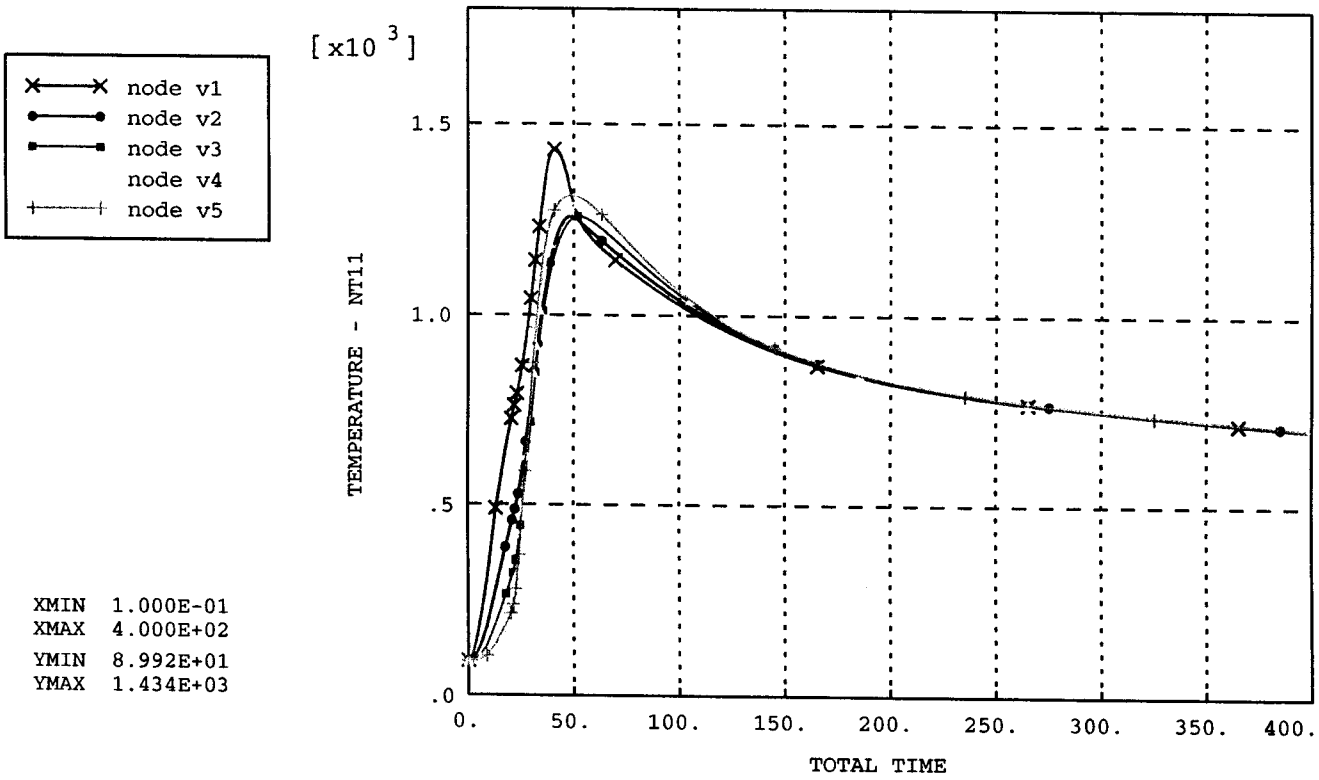

Fig. 5 Continued. Temperature distribution: **(b)** across the thickness

final stabilizing temperature of the weldment. An initial length over which the AHI is applied is assumed to be L_0 and is incremented while checking for the final stabilizing temperature of the weldment. This stabilizing temperature is compared with a predetermined value, and the incrementation is continued until the final stabilizing temperature is within the range of this predetermined value. When a final value of length is obtained, the value is passed on to the function, which is used to determine the magnitude of the AHI (step 1). When the subroutine completes this step, an optimized value of both length of application and magnitude corresponding to it will be achieved.

Step 3: Ramp Function. To optimize the ramp function, the following procedure was adopted. The rate of cooling of the weldment depends on the ramp function used for the AHI. To arrive at a suitable ramp function, section CD is considered. As one can see in Fig. 2, the locations of the heat inputs used are the AHI, which is applied on the top surface of the weldment, and the welding heat input, which is applied in the bottom surface. CD, a line passing through the midpoint along the thickness of the weldment, is considered to be a representative section, which would consider the heat effects from both the auxiliary and welding heat inputs.

During cooling, the time at which the temperature of the fusion zone (FZ) reached T_z (about 310.778 K (100 °F) below melting point) is recorded. The cooling rate at every node along CD was measured at the recorded time. The maximum value of the difference in cooling between point C and the other points along CD (dt_u) was evaluated. The total time of application of the ramp function is changed incrementally so that the dt_u is reduced. This is continued until dt_u is converged.

The value of the total time of application of AHI which was obtained is passed on to the length function (step 2), to obtain the optimized value of length of application of the AHI for this total time. The length function in turn calls the magnitude function (step 1) in a nested fashion to arrive at the optimized values of magnitude, length of application, and the total time of application of the AHI.

Step 4: Smoothing. The subroutine increments the factor of smoothing for the ramp function obtained and optimizes it. The convergence criterion for the smoothing of the ramp function is to arrive at a gradient of cooling rate dt_u, which is the minimum. The initial and final ramp functions arrived at after smoothing are shown in Fig. 6. At this step, the magnitude, length of application, and total time of the ramp function are well defined and optimized.

Step 5: Starting Time of the AHI. The time at which the AHI is activated (t_1) with respect to activation time of welding heat input (t_2) is called *dts* ($dts = t_2 - t_1$). For the purpose of the analysis, the nodes along the thickness of the weldment (V_2, V_3, V_4 and V_5), including the node which is in contact with the AHI (v1), are selected. The area in which these nodes are located is considered to be most sensitive with respect to *dts*, because this section lies between the zones of heat transfer of the AHI and the welding heat input and serves as a representative section for this part of the analysis. The time at which the selected nodes in the weldment reach their respective peaks is considered to be the criterion used to achieve this end. The maximum difference in the times at which different nodes across the thickness reach their respective peaks is calculated (*dt*). The objective of this part of the subroutine is to arrive at an optimum value of *dts* for which *dt* is minimum. As an initial step, *dts* was set to zero. The time *dts* is incrementally

changed depending upon the value of *dt*, reducing *dt* at each increment. When the sign changes (*i.e*, an overshoot occurs) in any direction, the previous increment value is subtracted and an increment equal to one-tenth of the previous value is applied. This is repeated until a predetermined convergence in the value of *dt* is reached. This part is not coupled with other parts of the subroutine, which are responsible for changing the value of the AHI. The starting time of the AHI with respect to the welding heat input does not affect the AHI, but plays an important role in decreasing the temporal temperature distribution of the weldment.

3.2 Results of the Subroutine

This method was tried for two different cases: (a) T_s = 644.1 K (700 °F) and (b) T_s = 699.7 K (800 °F).

For case a. AHI heat = 8.831×10^5 kg/s^3 (0.54 Btu/in.^{2}/s); it is 1 in length and must be activated 21 s before welding torch, and the total time of activation is 50 s; the time function ramp is shown in Fig. 6.

For case b. AHI heat = 1.014×10^6 kg/s^3(0.62 Btu/in.^{2}/s); it is 0.037 to 0.038 m (1.46 to ~1.5 in.) in length, must be activated 23 s before welding torch, and the total time of activation is 54 s.

This method was tried for T_s = 838.6 K (1050 °F) (0.05 m or 2 in., AHI); however, in the discussion of the results, only cases a and b are emphasized.

4. Discussion of Results

When the numerical analysis that was done initially without the AHI is compared with the experimental analysis of Shim's results (Ref 12) in Fig. 1, a close agreement between both analyses is observed.

When an arbitrary AHI was selected (Fig. 5a), a thermal shock across the thickness of the weldment was introduced. This called for defining a criterion for selecting an appropriate AHI. Analysis following use of the technique mentioned in Section 3 showed that the transient and spatial temperature gradient in the weldment was reduced, which resulted in reduced residual stresses.

Figure 5(b) shows the temperature distribution across the thickness when the analysis was done by the proper selection of the AHI. When Fig. 5(a) and (b) are compared, it can be seen that, by proper selection of the AHI, V_1 and the other nodes reach their peaks at the same time; furthermore, the spatial temperature gradient is drastically reduced.

Consideration of the peak temperature difference between v1 and the other nodes is important for two reasons: first, because V_1, V_2, V_3, V_4 and V_5 are across the thickness of the plate and a high spatial and temporal temperature gradient across the thickness may result in internal cracking in the weldment; and second, because V_1 is in the area where the AHI is applied. This peak temperature difference is evidently greater when an arbitrary AHI is chosen (from Fig. 5a). The suitable selection of the AHI reduced the peak temperature difference not only between V_1 and the other nodes, but also between any two other nodes, such as V_3 and V_4, and so forth. This fact is clearly evident from Fig. 5(b).

Figures 7 and 8 show the speed of cooling of two points on the weldment (Z_2 and V_5 in Fig. 2) As one can see from the curve for 0 in. AHI in Fig. 7, the cooling rate varied from about –13 to about –2 in 50 s. However, when 0.025 m (1 in.) AHI was used, the rate of cooling varied from –11.5 to about –4 in the same time span of 50 s. This indicates that when no auxiliary heat source is used, a sharp transient temperature gradient occurs during air cooling.

The curve for 0.038 m (1.5 in.) AHI shows a variation in cooling rate from –9 to to –4 in about 50 s, and the curve for 0.05 m (2 in.) AHI shows a variation from –7.5 to –3.5 in 50 s time span. This clearly indicates that, as the magnitude of AHI increased, the cooling rate decreased.

The peak cooling rate for 0 in. AHI is about –13, which reduced to around –11.7 when 0.025 m (1 in.) AHI was used. The

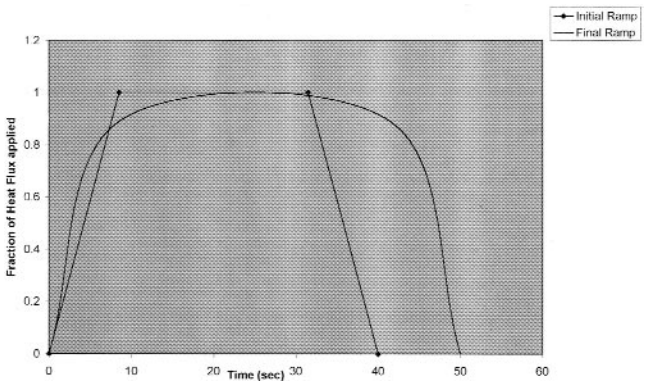

Fig. 6 Modification of ramp function

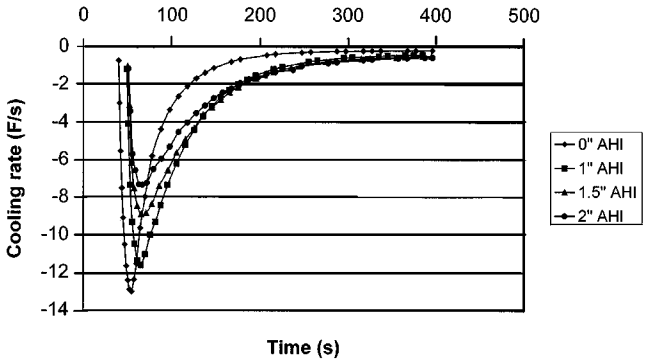

Fig. 7 Cooling rate vs time for node Z_2

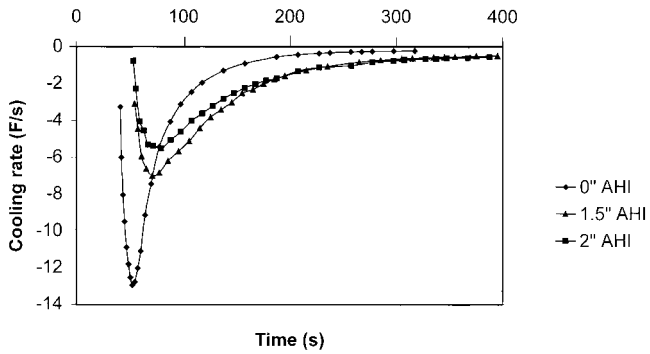

Fig. 8 Cooling rate vs time for node V_5

rate was further reduced to about –9 with 0.038 m (1.5 in.) AHI, and the trend continued with the increase in the AHI. From this discussion, one can conclude that the speed of cooling at point Z_2, which is close to the FZ, reduced and became more uniform as the size of AHI increased (Fig. 7).

In Fig. 8, the same trend is observed, but the peak cooling rate value further decreased, indicating a more uniform rate of cooling. This also indicates that, as one moves away from the heat inputs, the cooling rate further decreases.

Figure 9 shows the transient temperature distribution at the FZ and HAZ areas. In these figures, every node in the FZ and HAZ is selected and its temperature distribution versus time is plotted. These sets of nodes are labeled as HO, as indicated in the legend appearing in the graphs.

Figure 9(a) shows the temperature distribution without AHI. One can observe a very sharp transient temperature gradient. In Fig. 9(a), the temperature dropped from about 2.75×10^3 K (4500 °F) to about 533 K (500 °F) within 70 s. When the maximum temperature of the FZ and HAZ drops below 810.8 K (1000 °F) at t = 50 s, a relatively high spatial temperature gradient can be observed. Finally, the stabilizing temperature is 430.2 K (315 °F) after 400 s.

Figures 9(b) and (c) show the temperature distribution with AHI = 0.025 m (1 in.) and AHI = 0.038 m (1.5 in.), respectively. One can observe that the sharp transient temperature gradient of Fig. 9(a) has changed to a smoother curve in Fig. 9(b) and (c). In Fig. 9(b), the temperature dropped from about 2.9×10^3 K (4800 °F) to about 810.8 K (1000 °F) within 100 s. In Fig. 9(c), the temperature dropped from about 2.97×10^3 K (4900 °F) to about 810.8 K (1000 °F) within 170 s. The spatial temperature gradient, when the maximum temperature in Fig. 9(b) and (c) dropped below 1.09×10^3 K (1500 °F), is high when compared with the rest of the curve. However, when compared with the spatial temperature gradient of Fig. 9(a), a decrease in the cooling rate can be observed.

The peak temperature in Fig. 9(a) when no AHI was used increased from 2.75 to 2.9×10^3 K (4500 to 4800 °F) when 0.025 m (1 in.) AHI was used in Fig. 9(b); when the AHI used was 0.038 m (1.5 in.), it further increased to about 2.97×10^3 K (4900 °F). As the AHI was increased, the peak temperature of the distribution increased, which might not be desirable when the temperature gradient is considered. However, when compared with the increase in the stabilizing temperature and the gradual decrease in the cooling rate, the rise in the peak temperature is favorable rather than detrimental.

When an initial AHI was chosen both at the FZ and HAZ, there was an increase in the stabilizing temperature. The stabilizing temperature was obtained for an arbitrary AHI. A subroutine was developed and used to obtain the AHI when the stabilizing temperature was about 644.1 K (700 °F), which is around the A3 temperature, and the magnitude, the starting time, and the length over which the AHI is to be applied were obtained as explained

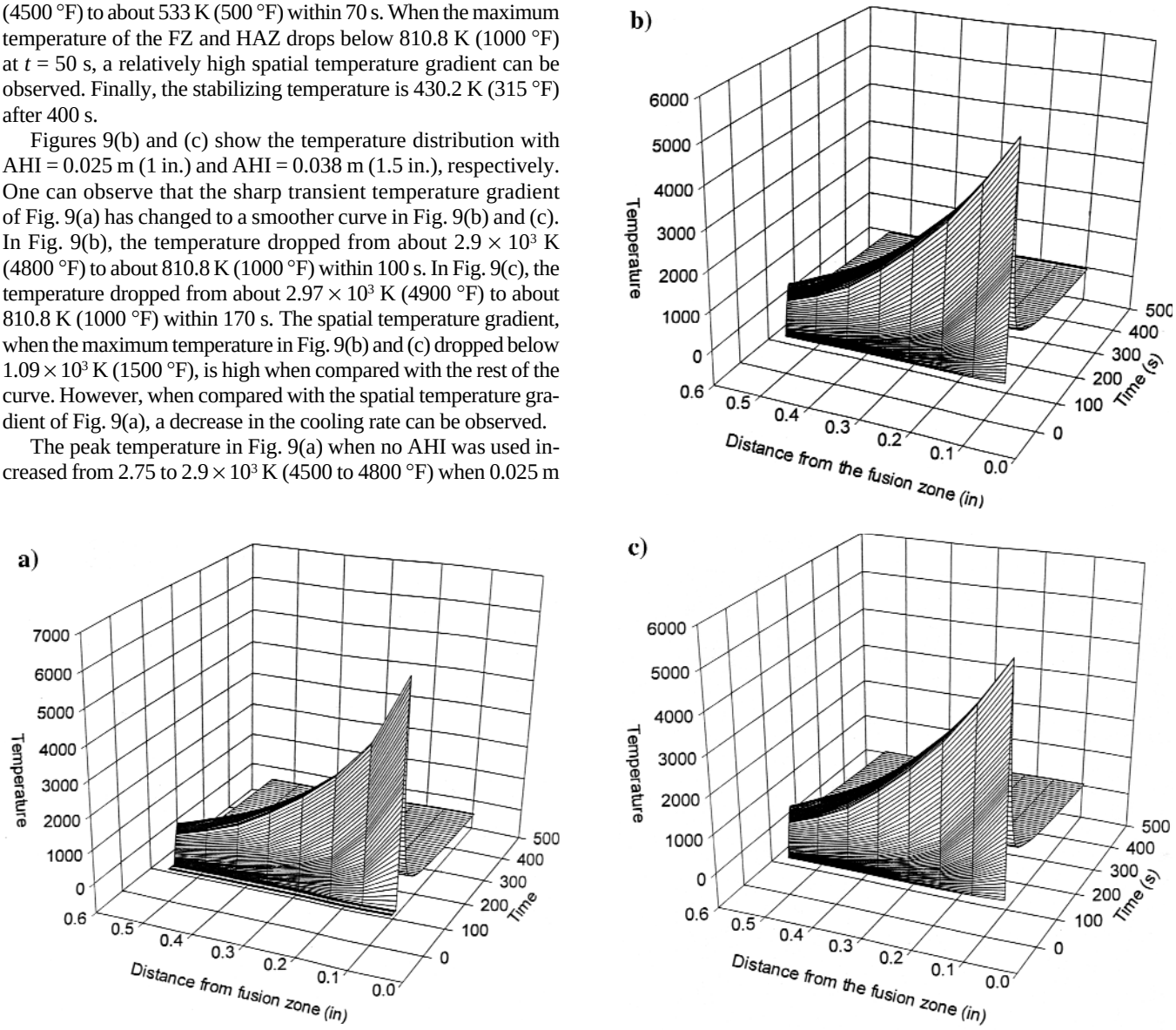

Fig. 9 Temperature distribution across line 3: **(a)** AHS = 0 in., **(b)** AHS 1 = in., and **(c)** AHS = 2 in.

in Section 3. The temperature distribution using this AHI is as shown in Fig. 9(b). The AHI arrived at resulted not only in the increase in the stabilizing temperature, but also brought about a gradual decrease in the rate of cooling (Fig. 9). In Fig. 9(c), the temperature distribution, with an AHI that was obtained for another value of stabilizing temperature 699.7 K (800 °F), is depicted.

Figure 10 shows the temperature contour plots when the maximum temperature of the FZ dropped into the neighborhood of 1.89×10^3 K (2950 °F) (310.78 K, or ~ 100 to ~ 150 °F, above melting point). The spatial temperature gradient obtained when no AHI is used is 4.134×10^4/m (1430 °F/in.), as shown in the calculations in Fig 10(a). It reduced to 2.76×10^4 K/m (802.4 °F/in.) (Fig. 10b) when 0.025 m (1 in.) AHI was used. When 0.038 m (1.5 in.) AHI is used, as shown in Fig. 10(c), it was further reduced to 2.64×10^4 K/m (748.43 °F/in.).

These plots were obtained within the first 40 s of the analysis, one-tenth of the total time of the analysis.

Figure 11 shows the temperature contour plots after 400 s. One can clearly observe that the stabilizing temperature when no AHI was used was about 424.1 K (304 °F), as shown in Fig. 11 (a). When AHI increased to 0.025 m (1 in.), the stabilizing temperature increased to 697, nearing 644.1 K (700 °F) (Fig. 11b); and, on further incrementation of the AHI to 0.038 m (1.5 in.) (Fig 11c), the stabilizing temperature reached a value of 706.9 K (813 °F), which is around 699.7 K (800 °F). The authors have tabulated their findings in Table 1.

These results indicate that the temperature distribution, spatially and temporally, becomes more uniform when an AHI of sufficient magnitude, ramp function, and optimum length is arrived at by following a procedure such as the one described in the subroutine. Uniform temperature distribution is a desirable result as far as stress distribution is concerned. Since the temperature gradient is reduced, and considerable time is given for stress relief, a weldment with reduced residual stresses as compared with the conventional welding procedure is expected.

5. Conclusions

Scrutinizing the results of Table 1 and Fig. 1 to 11, the following conclusions may be drawn.

- During conventional gas metal arc welding, a high spatial temperature gradient exists at the area close to the HAZ; rapid and nonuniform speed of cooling is also observed close to the HAZ.
- By selecting an arbitrary heat source without carefully examining the theory behind it, thermal shock will almost certainly be introduced into the plate.
- By introducing an appropriate AHI, the speed of cooling is reduced, and it also becomes more uniform. This will result in reduced residual stresses.

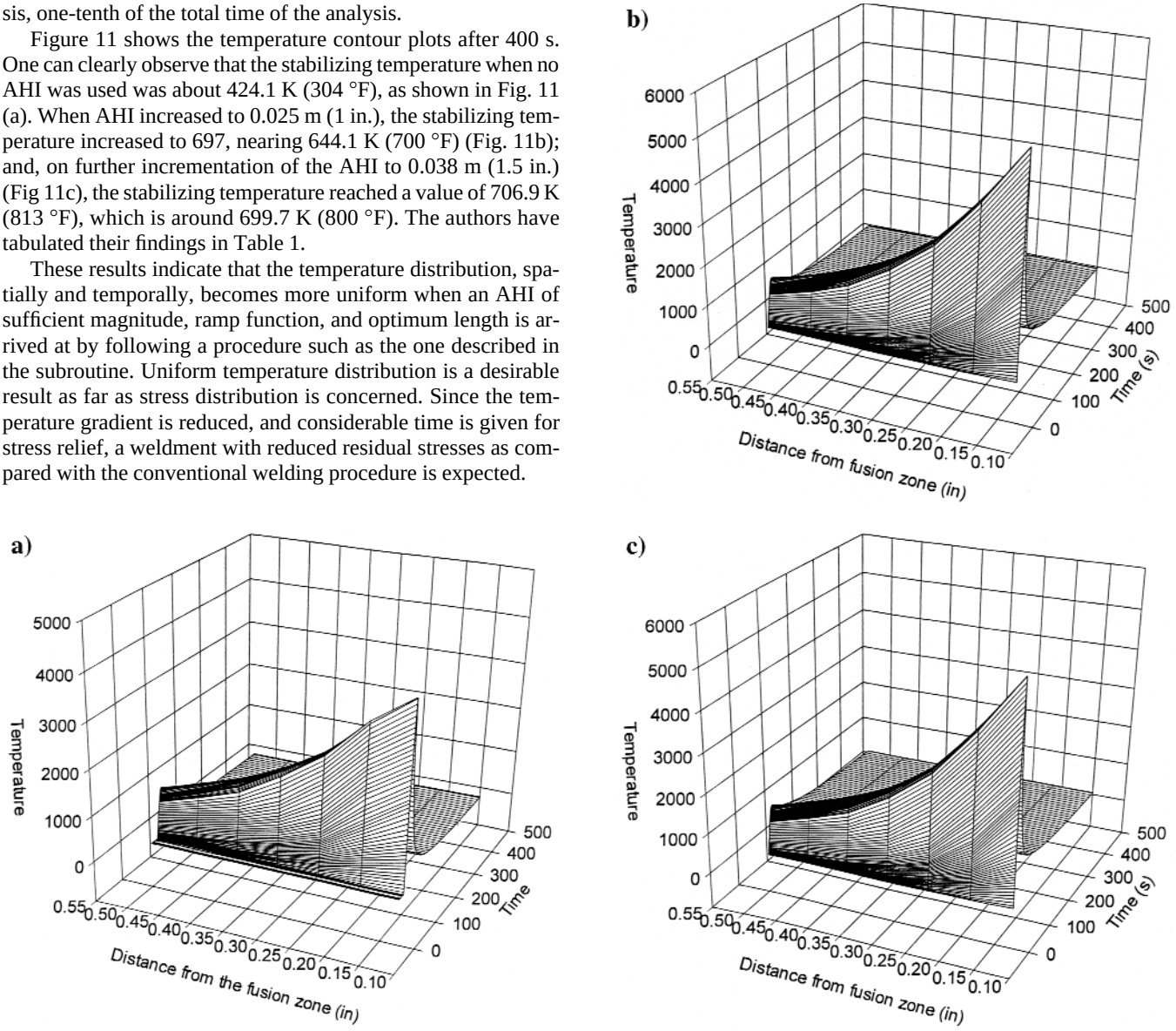

Fig. 10 Temperature distribution across line 4: **(a)** AHI = 0 in., **(b)** AHI = 1 in., and **(c)** AHI= 2 in.

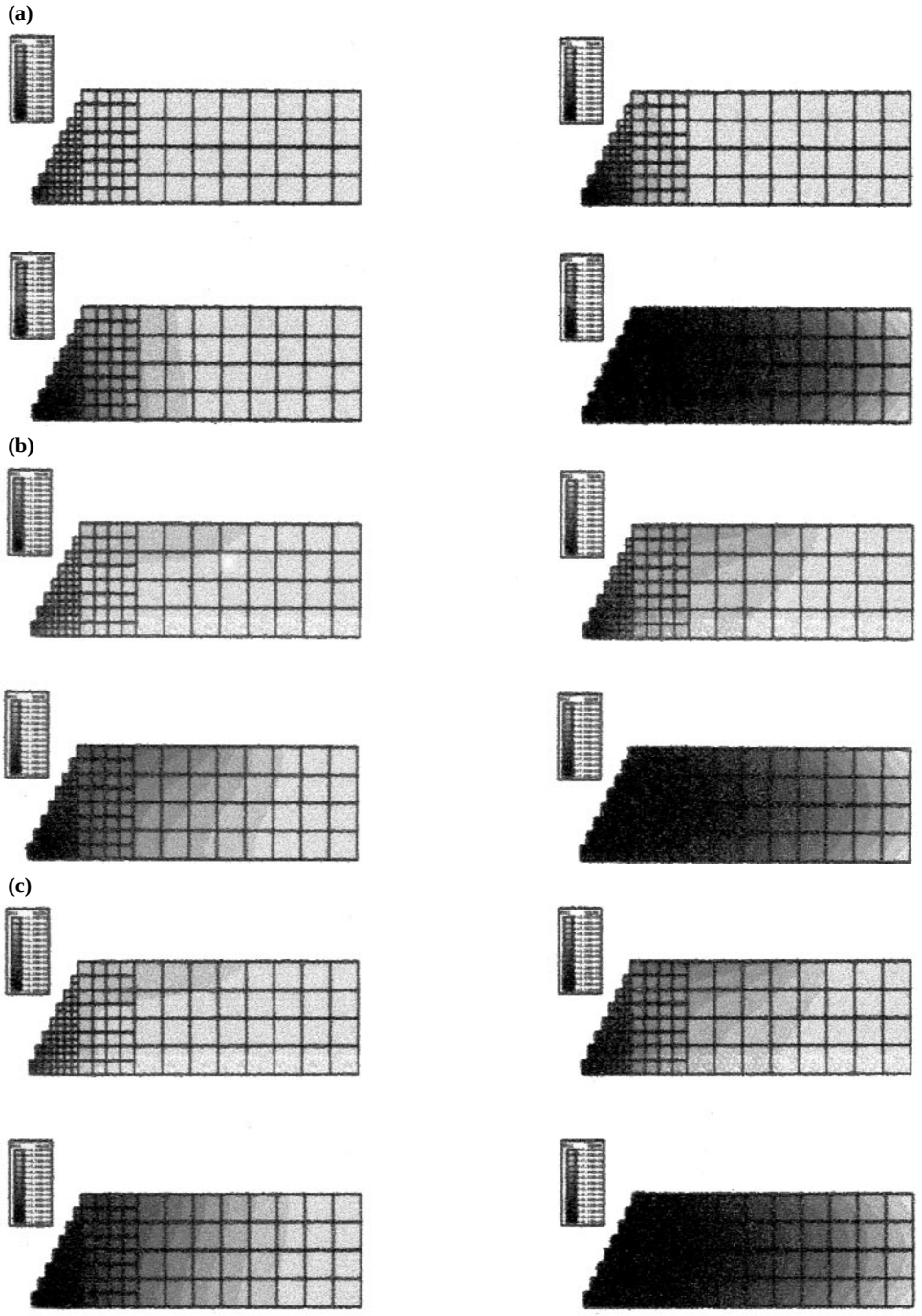

Fig. 11 Temperature contour plot after 400 s showing stabilizing temperature: **(a)** AHS = 0 in., **(b)** AHS = 1 in., and **(c)** AHS = 1.5 in. **(a)** Temperature contour plot after 400 s showing stabilizing temperature. AHS = 0 in . **(b)** Temperature contour plot after 400 s showing stabilizing temperature. AHS = 1 in. **(c)** Temperature contour plot after 400 s showing stabilizing temperature. AHS = 1.5 in.

- By selecting an appropriate stabilizing temperature and air cooling the entire weldment from that temperature, the residual stresses may be relieved.

Acknowledgments

Part of this research was completed with the assistance of grants from the Society of Manufacturing Engineers (SME) (Grant No. 598-2449) and the Research Incentive Fund (RIF) of Temple University. The authors greatly appreciate the funding of the SME and RIF.

References

1. Y. Ueda, K. Nakacho, and T. Shimizu: *J. Pressure Vessel Technol.*, 1986, vol. 108, pp. 14-23.

Table 1 Comparison of Conventional GMAW with GMAW with well defined AHI

	Spatial temperature gradient, *dT/dX*	Average speed of cooling at the HAZ and FZ(a), *dT/dt*	Stabilizing Temperature(b), T_s
Case A Conventional GMAW process	4.134×10^4 K/m (1430 °F/in.) The spatial temperature gradient was measured when the maximum temperature of the FZ and HAZ dropped to 1.89×10^3 K (2950 °F). See Fig. 10(a)	320.2 K/s (117×F/s) At this time (t = 50 s), the temperature distribution at the HAZ and FZ varies between 677.4 and 1033 K. See Fig. 9(a)	427.2-433 K (320-310 °F) See Fig. 11a
Case B Conventional GMAW with well-defined AHI over a length of 1 in.	2.76×10^4 K/m (802.4 °F/in.) The spatial temperature gradient was measured when the maximum temperature of the FZ and HAZ dropped to 1.9×10^3 K (2960 °F). See Fig. 10(b).	271 K/s (28.5×F/s) At this time (t = 170 s), the temperature distribution at the HAZ and FZ varies between 827.4 and 794.1 K. See Fig. 9(b).	691.3-685.8 K (785-775 °F) See Fig.11b
Case C Coventional GMAW with well-defined AHI over a length of 1.5 in.	2.6×10^4 K/m(743 °F/in.) The spatial temperature gradient was measured when the maximum temperature of the FZ and HAZ dropped to 1866 K (2900 °F). See Fig. 10(c)	262.9 K/s (13.8 °F/s) At this time (t = 280 s), the temperature distribution at the HAZ and FZ varies between 810.8 and 820. See Fig. 9(c)	750.8-748 K (892-887 °F) See Fig. 11c
Case D Conventional GMAW with arbitrary AHI	See Fig. 5	. . .	. . .

GMAW, gas metal arc welding. (a) When the average temperature at those areas dropped below 810.8 K (1000 °F). The average speed of cooling at the HAZ and FZ was evaluated by subtracting the maximum temperature at the FZ and HAZ from 1000°F, divided by the average time that the average temperature of the FZ and HAZ took to drop below 1000 °F. (b) After 400 s, the temperature of the entire plate from the heat source up to 6 in. was stabilized.

2. A. K. Bhadwi, S. Sujith, G. Srinivasan, T.P.S. Gill, and S.L. Mannan: *Weld. Res. Suppl.*, 1995, pp. 153s-158s.
3. C.P. Chou and Y.C. Lin: *Mater. Sci. Technol.*, 1992, vol. 8, pp. 179-83.
4. Y.C. Lin and C.P. Chou: *Mater. Sci. Technol.*, 1992, vol. 8, pp. 837-40.
5. Y.C. Lin and C.P. Chou: *Mater. Processing Technol.*, 1995, vol. 48, pp. 693-98.
6. K.C. Chang and C.P. Chou: *Weld. Cutting*, 1995, vol. 5, pp. 1-6.
7. Y.C. Lin and K.H. Lee: *Int. J. Pressure Vessels Piping*, 1997, vol. 71, pp. 197-202.
8. S. Jahanian: *J. Thermal Stresses*, 1996, vol. 19, pp. 513-29.
9. S. Jahanian and M. Sabbaghian: *J. Pressure Vessel Technol.*, 1990, vol. 112, pp. 85-91.
10. S. Jahanian and M. Tavakoli: *Mater. High Temp.*, 1998, vol. 15, pp. 29-33.
11. R.R. Kunde, P.V. Kuppa, and S. Jahanian: *Reliability, Stress Analysis and Failure Prevention Aspect of Adhesive and Bolted Joints and Rubber Components*, E. Sancaktar, ed., IMECE, Los Angeles, CA, 1998, DE-Vol. 100, pp. 151-59.
12. Y.L. Shim: Ph.D. Thesis, Ohio State University, Columbus, OH, 1992.